CFD analysis of a thermal storage tank driven by natural convection

Germilly Barreto[1], José González-Aguilar[1], Manuel Romero[1] and Alberto Giaconia [2]

[1]High Temperature Processes Unit, IMDEA Energy, Avda. Ramón de la Sagra 3, 28935, Móstoles, Spain

[2]ENEA, Casaccia Research Center, Via Anguillarese, 301, 00123 Rome, Italy

Abstract

This work addresses a numerical research on a concept of thermal energy storage tank by natural convection. The design of the tank comprises a single reservoir with molten salt and two indirect heat exchangers (thermal oil to molten salt) inside. For discharging, cold thermal oil circulates in the heat exchanger located at the top of the tank, and due to natural convection, the cooled molten salt moves to the bottom of the tank through an adiabatic channel. For charging, the hot thermal oil circulates through the bottom heat exchanger, heating the molten salt and causing it to move up through a second channel. To analyze this concept, a two-dimensional computational fluid dynamics (CFD) model is developed and used to investigate the storage system for different discharge and charge conditions of the heat exchangers. The mass flow rate of the molten salt in the channels, inlet and outlet temperatures of the heat exchangers, and temperature and velocity distribution in the tank are analyzed for different imposed resistance of the flow and discharge/charge rate of the heat exchangers. As main results, the pattern of the mass flow rate of the molten salt in the channels are identified, and its magnitude depends on the design of the heat exchanger, temperature, and heat sink/source. The evolution of the inlet and outlet temperature in the heat exchangers are key indicators to identify the discharge and charge duration of the thermal storage tank and assessing its potential to work as a thermocline system.

Keywords: thermal energy storage, natural convection, numerical modelling, CFD

1. Introduction

To foster the adoption of medium- and high-temperature solar thermal technologies, it is fundamental to implement low-cost thermal storage systems. For this reason, the possibility of using a single stratified tank containing molten salt and driven by natural convection is being analyzed. This concept might avoid costs associated with external pumping of molten salt and control. In this regard, Russo et al. (2018) analyzed this concept integrated into a plant with a solar field and an organic Rankine cycle using a simplified numerical approach. They found that controlling the mass flow rate of molten salt in the tank was necessary for the correct operation of the integrated system. On the experimental side, Gaggioli et al. (2020) conducted an experimental campaign to characterize this concept integrated with real operating conditions, analyzing both discharge and charge modes. For both modes, they found that while the storage system can maintain appropriate temperatures, the minimum temperature during discharge and the maximum temperature during charging were never reached. They concluded that this was related to the high speed of molten salt in the channels. Recently, Cagnoli et al. (2023) developed and validated a transient 2D axisymmetric computational fluid dynamics (CFD) model and used it to analyze the discharging and charging processes to determine heat losses and temperature distribution in the tank. They also investigated numerically the effect of the diameter of the internal channel on the performance of the tank, finding that decreasing the diameter leads to an increase in the temperature of the molten salt. Mostly, for analyzing thermal energy storage systems, particularly thermoclines, the key performance indicators include the time evolution of temperature distribution within tank and discharge/charge efficiency. For example, Shokrnia et al. (2024) employed a 2D axisymmetric CFD model validated with experiments to investigate performance improvement in the storage tank through the incorporation of phase change materials (PCM). Their modifications demonstrated a significant increase in storage capacity, discharge and charge efficiency, and improved temperature distribution. However, literature

Selection and/or peer review under responsibility of Scientific Committee
10.18086/eurosun.2024.06.05 Available at http://proceedings.ises.org

on this thermal storage system concept consistently highlights the critical role of the mass flow rate within the channels. Detailed analyses to assess the behavior of this type of storage tank, where natural convection may promote undesirable flow patterns, are lacking in the literature. To address the gap of knowledge, this work develops a two-dimensional CFD model and uses it to analyze the discharging and charging cases for different working conditions of the heat exchangers. The flow rate of the molten salt in the channel, inlet and outlet temperature in the heat exchangers, and the distribution of temperature and molten salt velocity in the tank are assessed.

2. Thermal energy storage design

The main components and working principle for discharging and charging in this concept of thermal storage tank are presented in Figure 1. For discharging, cold thermal oil circulates in a heat exchanger located on the top of the tank (HEx1), which cools down the molten salt and increases its density. Due to natural convection, the cooled molten salt flows to the bottom of the tank through an adiabatic channel (a cylindrical shell crossing the thermocline layers in the vertical direction). For charging, the hot thermal oil (from a solar field) circulates in the heat exchanger at the bottom of the tank (HEx2), which heats up the molten salt and decrease its density. This causes the molten salt to rise to the top of the tank through the charge channel.

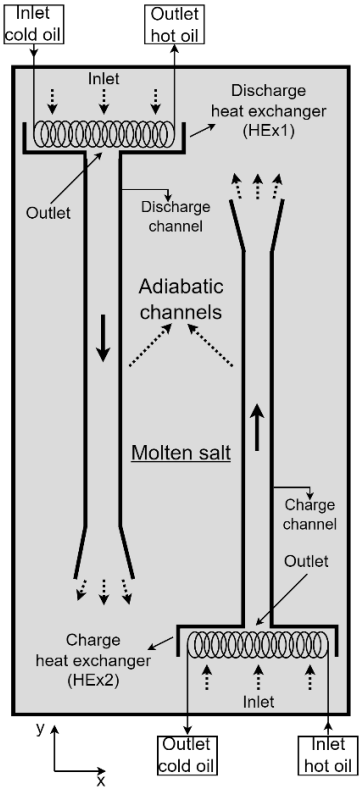

Fig. 1: Two-dimensional scheme of the thermal storage tank driven by natural convection.

3. Numerical modelling

The conservation equations for mass, momentum and energy were solved in Cartesian coordinates using finite element method (FEM) in COMSOL Multiphysics (v6.1),

$$\rho \frac{\partial}{\partial t} + \nabla \cdot (\rho \mathbf{u}) = 0 \qquad \text{(eq. 1)}$$

$$\rho \frac{\partial \mathbf{u}}{\partial t} + \rho(\mathbf{u} \cdot \nabla)\mathbf{u} = -p\nabla + \nabla \cdot \left(\mu(\nabla \mathbf{u} + (\nabla \mathbf{u})^T) - \frac{2}{3}\mu(\nabla \mathbf{u})\mathbf{I}\right) + \left(\rho - \rho_{ref}\right)\mathbf{g} - \mathbf{F} \qquad \text{(eq. 2)}$$

$$c_p \frac{\partial T}{\partial t} + \rho c_p \mathbf{u} \cdot \nabla T = \nabla \cdot (k \nabla T) + Q \qquad \text{(eq. 3)}$$

where ρ, c_p, μ and λ are the density, heat capacity, dynamic viscosity and thermal conductivity of the molten salt, **u** is the velocity vector, p is the pressure, T is the temperature, respectively, and **g** is the gravity acceleration. The heat exchangers are modelled considering a momentum sink **F** in the momentum conservation equation and a heat sink/source Q in the energy conservation equation. The heat sink (negative value) is used for simulate the discharge and a heat source (positive value) is used for the charge and expressed as,

$$Q = Q_0 + m\,t \qquad \text{(eq. 4)}$$

The following formulation for the momentum source is used in the heat exchanger domain:

$$\mathbf{F} = -C_1 \mu \mathbf{u} \qquad \text{(eq. 5)}$$

where C_1 is a momentum sink coefficient. The fluid considered in this study is the molten salt Hitec XL (Na/K/Ca nitrate), with the temperature dependence of its thermal and hydrodynamic properties modelled. The temperature dependence of the fluid density, heat capacity and dynamic viscosity are calculated using the correlations form the work of Giaconia et al. (2021).

3.1. Input parameters and boundary and initial conditions

The walls of the tank and channels are considered with non-slip boundary conditions for the fluid flow and as adiabatic for heat transfer. For discharge, the initial temperature of the tank is uniformly set to a hot temperature of 300 ℃, with a heat sink applied in the corresponding heat exchanger (HEx1), while the inlet of the charge heat exchanger (HEx2) is treated as a wall for fluid flow. For charge, the initial temperature of the tank is uniformly set to a cold temperature of 290 ℃, with a heat source applied in the corresponding heat exchanger (HEx2), while the inlet of the discharge heat exchanger (HEx1) is treated as a wall for fluid flow. Table 1 shows all the main parameters used in this analysis.

Tab. 1: Main geometric parameters of the thermal storage tank.

Description	Dimensions (cm)
Height of the tank	171
Width of the tank	80
Height of heat exchanger	8
Width of the heat exchanger	38
Width of the discharge channel	10
Width of the charge channel	6

4. Results

To check the robustness of the numerical model, the evolution of the computed inlet and outlet mass flow rates in the heat exchangers are compared and maximum difference of less than 5% were found. Figure 2 and Figure 4 show the temperature (℃) distribution and flow direction in the tank at 0, 4, 8, 12, and 16 min (from left to right) during the discharge (Figure 2) and charge (Figure 4). Figure 3 and 5 show the time evolution of the molten salt mass flow rate in the channel (figure on the right) and the inlet and outlet temperatures of the molten salt (figure on the right) in the discharge and charge heat exchangers, respectively. It is observed that for this type of thermal storage, the mass flow rate in the channel shows three main stages during discharging. The first stage consists of a rapid increase in the mass flow rate until it reaches a maximum value (within the first minute), followed by a decrease until a stable region is reached, and finally a third stage characterized by a more stable zone. This instability of the mass flow rate in the channel have also been raised in other works present in literature, such as the study of Gaggioli et al. (2020). Regarding the inlet and outlet temperatures, the outlet exhibits significant fluctuation due to the unstable flow in the channels.

Fig. 2: Temperature (°C) distribution and flow direction in the tank for different times during discharge (heat sink of 1 MW m^{-3} and no momentum sink in the heat exchanger).

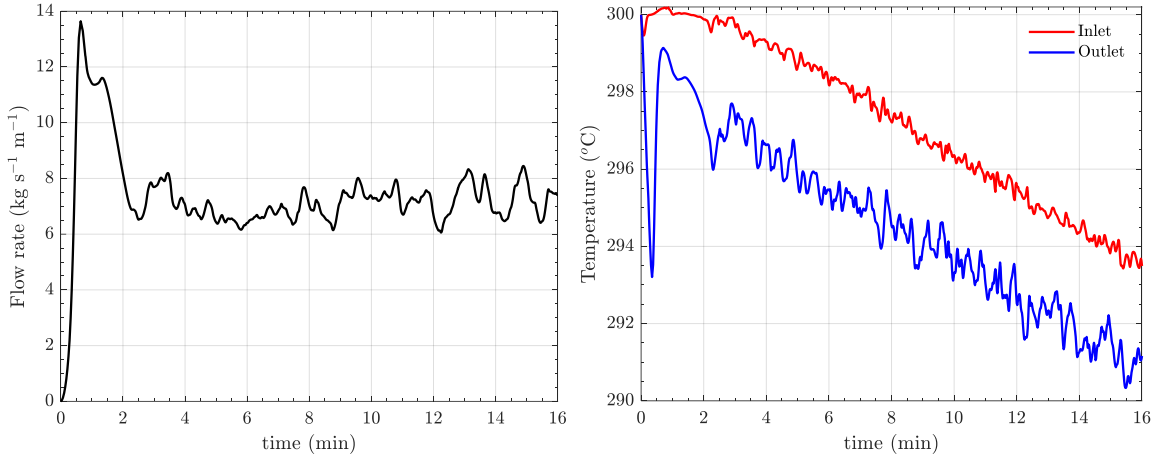

Fig. 3: (left) Mass flow rate of the molten salt in the discharging channel and (right) inlet and outlet temperatures of the molten salt at the cold heat exchanger (heat sink of 1 MW m^{-3} and no momentum sink in the heat exchanger).

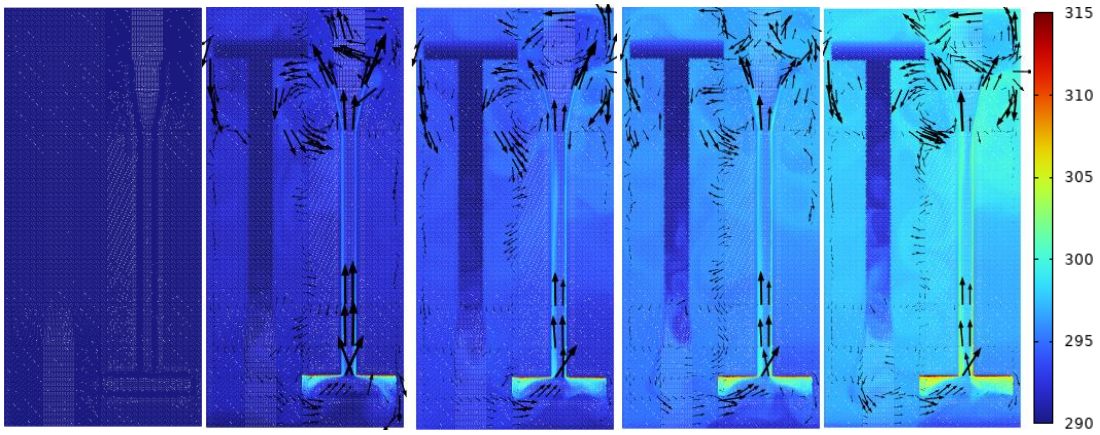

Fig. 4: Temperature (°C) distribution and flow direction in the tank for different times during charge (heat source of 1 MW m^{-3} and no momentum sink in the heat exchanger).

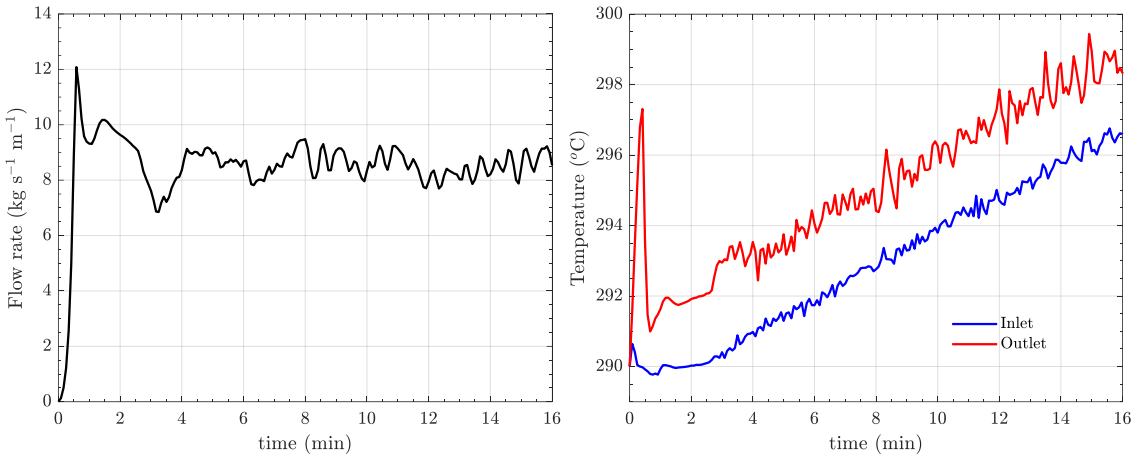

Fig. 5: (left) Mass flow rate of the molten salt in the charging channel and (right) inlet and outlet temperatures of the molten salt at the hot heat exchanger (heat source of 1 MW m^{-3} and no momentum sink in the heat exchanger).

4.1. Parametric analysis of discharge

In this section, a parametric analysis of the momentum sink coefficient C_1 and heat sink profiles during discharge of the thermal storage is presented. Figure 6 shows the evolution of the molten salt mass flow rate in the discharge channel for different momentum sink coefficient, while Figure 7 shows the corresponding inlet (left) and outlet (right) temperatures in the discharge heat exchanger. In both cases, a fixed heat sink of 1 MW m^{-3} was considered. The momentum sink coefficient introduces resistance to fluid flow in the discharge heat exchanger, resulting in a decrease in both the mass flow rate and its fluctuation within channel. This effect is directly correlated to the inlet and outlet temperatures in the heat exchanger, given a fixed heat sink. Although the different stages in the evolution of the mass flow rate in the channel remain, but lower peaks of mass flow rates are observed for higher momentum sink coefficients.

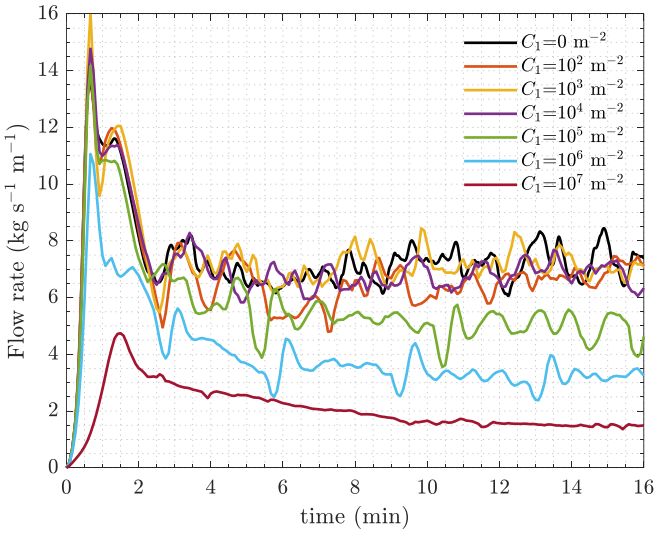

Fig. 6: Time evolution of the molten salt mass flow rate in the discharge channel for different momentum sink coefficient (heat sink, 1 MW m^{-3}).

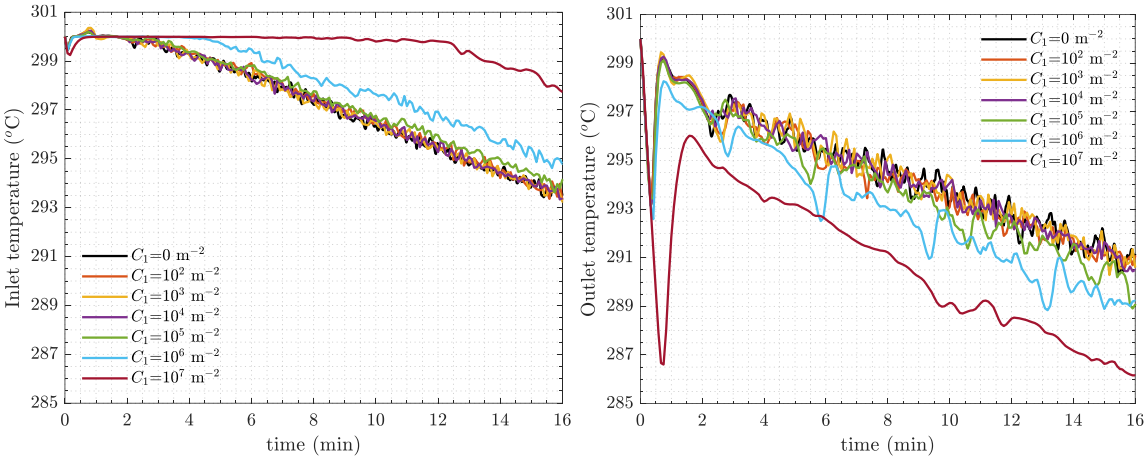

Fig. 7: Inlet (left) and outlet (right) temperatures in the discharge heat exchanger for different momentum sink coefficients (heat sink, 1 MW m^{-3}).

Regarding the use of different heat sink profiles for discharging, Figure 8 (left) shows the heat sink profiles used in the parametric analysis, while Figures 8 (right) shows the resulting evolution of the mass flow rate in the discharge channel, assuming a fixed momentum sink coefficient of 10^7 m^{-2}. Figure 9 presents the corresponding inlet (left) and outlet (right) temperatures in the discharge heat exchanger for the different heat sink profiles. It can be observed that increasing the slope of the discharging heat sink profile leads to more constant outlet temperature in the heat exchanger. This is an important finding, as demonstrates the potential of the thermal storage to behave as a typical thermocline system.

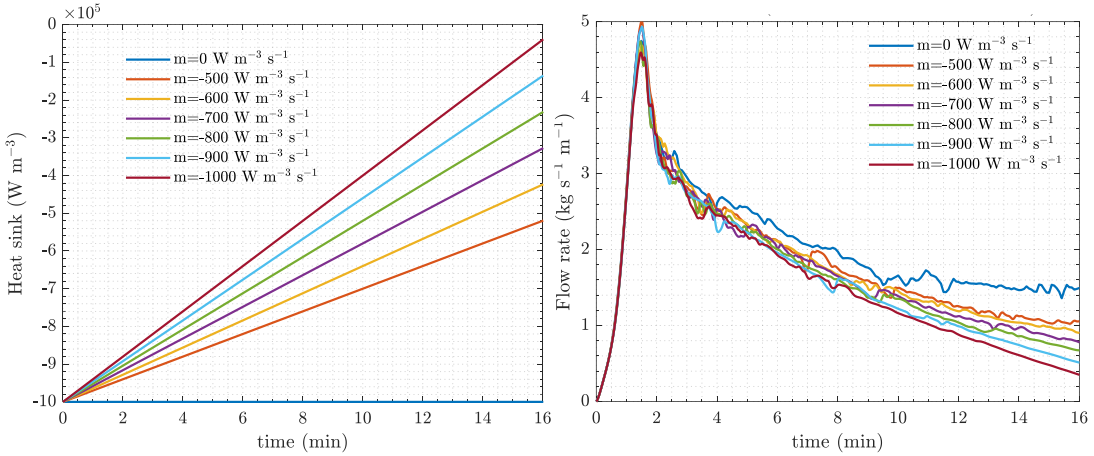

Fig. 8: Heat sink profiles (left) and the corresponding obtained mass flow rate (right) in the discharge channel ($C_1 = 10^7$ m^{-2}).

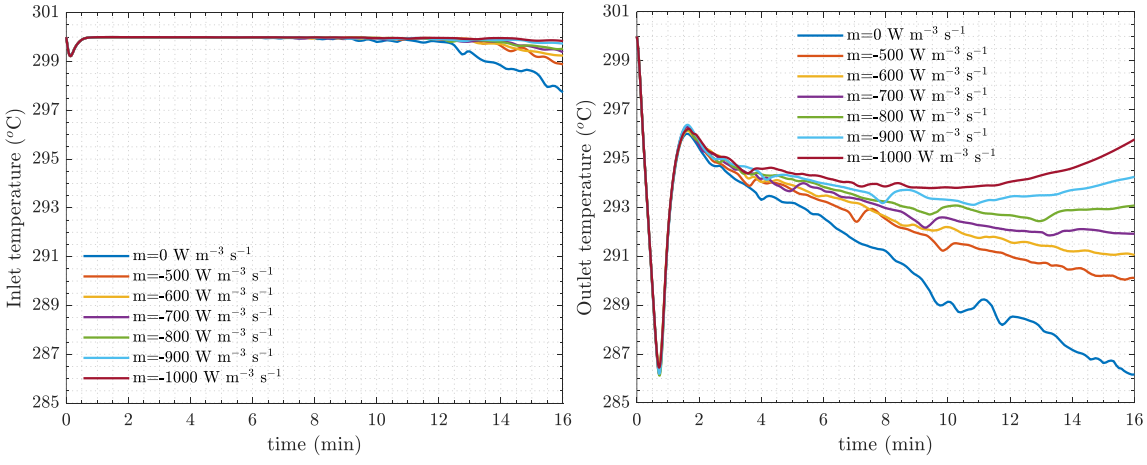

Fig. 9: Inlet (left) and outlet (right) temperatures in the discharge heat exchanger for different heat sink profiles ($C_1 = 10^7$ m^{-2}).

4.2. Parametric analysis of charge

For charging the tank, Figure 10 shows the evolution of the molten salt mass flow rate in the charge channel for different momentum sink coefficients, while Figure 11 illustrates the corresponding inlet (left) and outlet (right) temperatures in the heat exchanger. Both cases use a fixed heat source of 1 MW m^{-3}. The behavior is similar to that observed during discharge, with the peak of mass flow rate being less pronounced.

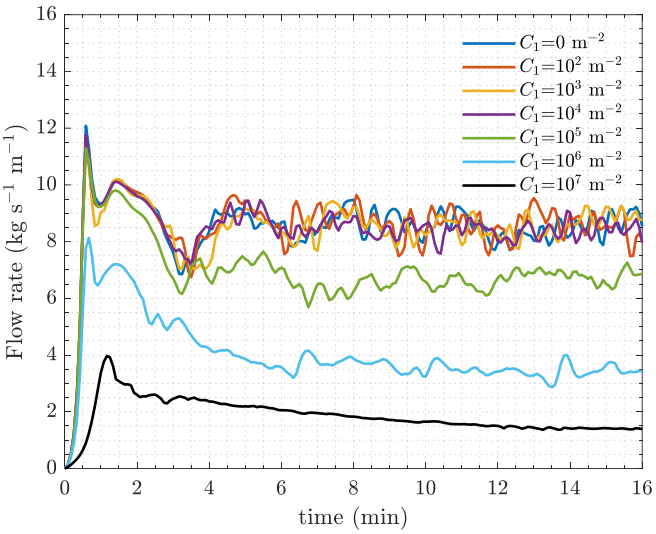

Fig. 10: Time evolution of the molten salt mass flow rate in the charge channel for different momentum sink coefficient (heat source, 1 MW m^{-3}).

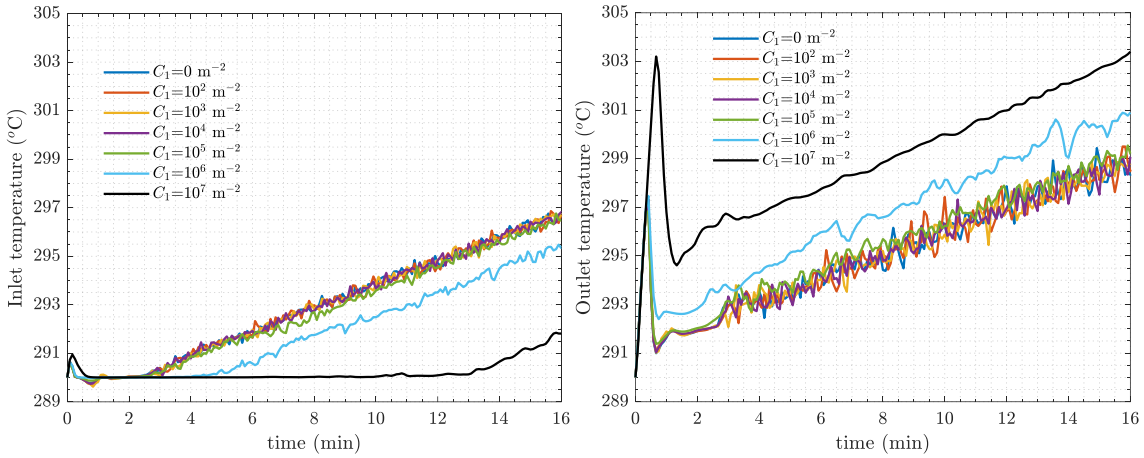

Fig. 11: Inlet (left) and outlet (right) temperatures in the charge heat exchanger for different momentum sink coefficients (heat source, 1 MW m^{-3}).

Regarding the heat source profile for charging, Figure 12 (left) shows the heat source profiles used in the parametric analysis, while Figures 12 (right) shows the resulted evolution of the mass flow rate in the charge channel, with a fixed momentum sink coefficient of 10^7 m^{-2}. Figure 13 shows the corresponding inlet (left) and outlet (right) temperatures in the charge heat exchanger for different heat source profiles. The same behavior observed in discharge mode is also present during charging, but the second stage of the decrease in the mass flow rate until a stable region less pronounced.

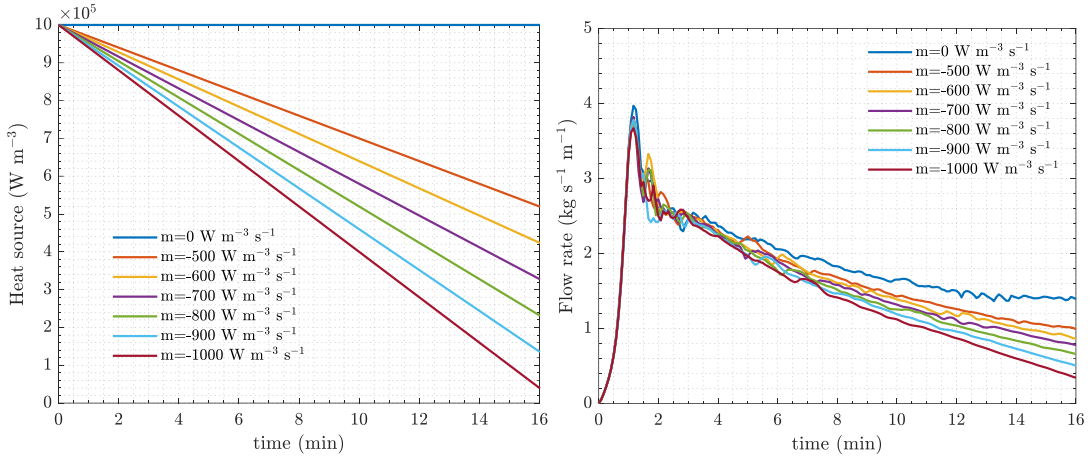

Fig. 12: Heat source profiles (left) and the obtained corresponding mass flow rate (right) in the charge channel ($C_1 = 10^7$ m^{-2}).

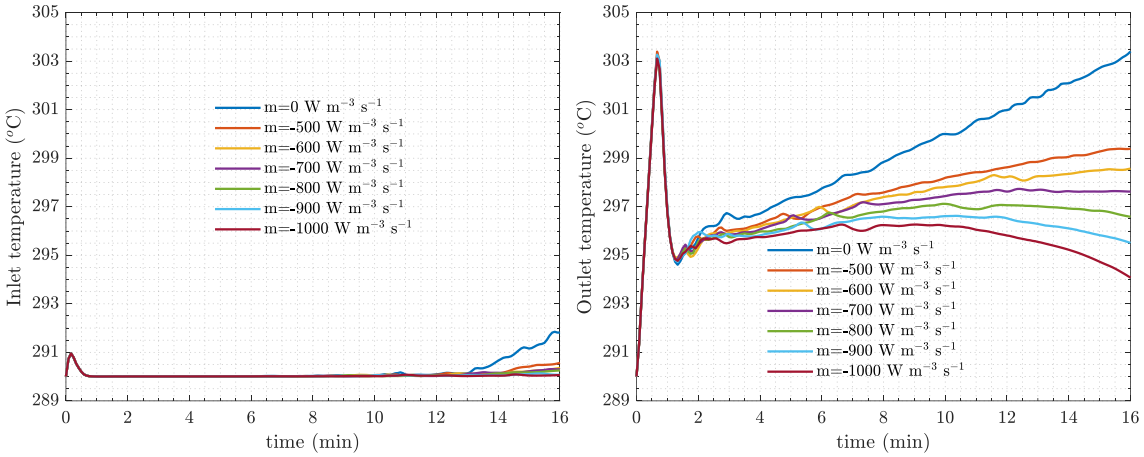

Fig. 13: Inlet (left) and outlet (right) temperatures in the charge heat exchanger for different heat sink profiles ($C_1 = 10^7$ m^{-2}).

5. Conclusions

This paper presents a numerical investigation of a concept for a thermal energy storage tank driven by natural convection. A two-dimensional CFD model is developed in COMSOL Multiphysics and used to analyze the storage concept in detail. First, a reference case with constant heat sink/source and no momentum sink in the heat exchanger is analyzed for both discharge and charge modes. It is observed that for this type of thermal storage, the mass flow rate in the channel exhibits three main stages during both discharge and charge. The first stage involves a rapid increase in the mass flow rate until it reaches a maximum value, followed by a decrease until a stable region is reached, and finally a third stage characterized by a more stable zone. The second stage is less significant in the charging case. The design of the heat exchanger plays a crucial role in the performance of this type of thermal storage, as it dictates the mass flow rate profile. From the analysis, it is found that a momentum sink coefficient of 10^7 and a heat sink slope of 800 W m^{-3} s^{-1} lead to a more constant outlet temperature of the molten salt in the discharge and charge heat exchangers, approaching behavior similar to that of a typical thermocline.

6. Acknowledgments

The authors would like to acknowledge the financial support and contributions from European Commission Horizon 2020 project PROMETEO (project reference number: 101007194) and the project partners' participation.

7. References

Cagnoli, M., Gaggioli, W., Liberatore, R., Russo, V., Zanino, R., 2023. CFD modelling of an indirect thermocline energy storage prototype for CSP applications. Solar Energy. 259, 86 - 98.

Gaggioli, W., Liberatore, R., Di Ascenzi, P., Mazzei, D., Russo, V., 2020. Experimental test of characterization of an innovative thermal energy storage system based on low melting molten salt thermocline tank integrated with an oil exchanger. SolarPACES 2019. 2303, 190012.

Giaconia, A., Tizzoni, A. C., Sau, S., Corsaro, N., Mansi, E., Spadoni, A., Delise, T., 2021. Assessment and Perspectives of Heat Transfer Fluids for CSP Applications. Energies. 14, 7486.

Russo, V., Mazzei, D., Liberatore, R., 2018. Thermal Energy Storage with Integrated Heat Exchangers Using Stratified Molten Salt System for 1 MWe CSP. SolarPACES 2017. 2033, 090025.

Shokrnia, M., Cagnoli, M., Gaggioli, W., Liberatore, R., Russo, V., Zanino, R., 2024.Geometrical and PCM optimization of a thermocline energy storage system. Journal of Energy Storage. 98, 113070.